The Palaeobotanist 63(2014): 113–126
0031–0174/2014

Petrography and Diagenesis of the Jurassic Jara Dome sandstones, Kachchh, Gujarat

SHAISTA KHAN* AND A.H.M. AHMAD

Department of Geology, Aligarh Muslim University, Aligarh 202002 (U.P), India.
**Corresponding author: shaista.khans03@gmail.com*

(Received 30 August, 2014; revised version accepted 11 September, 2014)

ABSTRACT

Khan S & Ahmad AHM 2014. Petrography and Diagenesis of the Jurassic Jara Dome sandstones, Kachchh, Gujarat. The Palaeobotanist 63(2): 113–126.

The sandstones of Ridge and Athleta members of Callovian and Oxfordian age exposed at Jara Kachchh, Gujarat have been studied for their petrography and diagenetic history. These sandstones are medium– to coarse–grained, moderately to well sorted, subangular to subrounded and show medium to low spherecity. These sandstones were derived from a mixed provenance including granites, granite–gneisses, low–and high grade metamorphic and some basic rocks of the Aravalli Range and Nagarparkar Massif.

A critical analysis of the various factors that have modified the original detrital composition of Ridge and Athleta sandstones indicates that tropical weathering under warm and humid conditions and long residence time at the sediment water interface in a shallow marine environment destroyed the labile grains and enriched the sandstones in quartz. The dominance of floating grains and point contacts in the sandstones indicate that detrital grains do not show much pressure affects is a result of either shallow burial or early cementation. The sandstones were cemented by iron oxide, carbonate, silica, dolomite, glauconite and clay in order of abundance at a depth of burial in the range of 670–2600 m and 762–2750 m.

Key–words—Detrital Mineralogy, Diagenesis, Jurassic, Jara Dome, Kachchh, Gujarat.

गुजरात में कच्छ के जुरासिक जारा डोम बालुकाश्म की शैलवर्णना एवं प्रसंघनन

शाइस्ता खान एवं ए.एच.एम. अहमद

सारांश

गुजरात के जारा कच्छ में अनावरित केलावियन व ऑक्सफोर्डियन के रिज़ व एथलिटा सदस्यों के बालुकाश्मों का उनकी शैलवर्णना एवं प्रसंघाती इतिहास हेतु अध्ययन किया जा चुका है। ये बालुकाश्म मध्यम से मोटे दाने, साधारणतः से सुनियत, अवकोणिक से उपगोलित और मध्यम से निम्न गोलाई दिखाते हैं। ये बालुकाश्म मिश्रित स्रोत जिसमें ग्रेनाईटीज़, ग्रेनाइट–नाइसिस, निम्न से उच्च ग्रेड मेटामॉर्फिक और अरावली रेंज एवं नागरपारकर मैसिफ की कुछ आधारित चट्टानें सम्मिलित हैं, से प्राप्त हुए थे।

विभिन्न कारकों का आलोचनात्मक विश्लेषण जिन्होंने रिज़ व एथलिटा बालुकाश्मों के वास्तविक अपरदी संयोजन को परिवर्तित किया, इंगित करता है कि उष्ण व आर्द्र स्थितियों के अंतर्गत उष्णकटिबंधीय अपक्षय तथा उथले समुद्री वातावरण में अवसाद जल अंतराफलक के दीर्घ वास समय पर अस्थिर दानों को नष्ट किया और क्वाटर्ज़ में बालुकाश्मों को उर्वर किया। बालुकाश्मों में प्लवमान दानों व बिन्दु संपर्कों की प्रमुखता इंगित करती है कि अपरदी दानों का अधिक दबाव प्रभाव नहीं दिखाता है जो कि या तो उथले शवाधान या प्रारंभिक सीमेन्टी भवन का परिणाम है। बालुकाश्मों को 670–2600 मीटर तथा 762–2750 मीटर की श्रेणी की गहराई में शवाधान की बाहुल्यता के लिए आयरन ऑक्साइड, कार्बोनेट, सिलिका, डोलोमाइट, ग्लोकोनाइट तथा मृदा द्वारा संयोजित किया गया था।

सूचक शब्द—अपरदी खनिज विज्ञान, प्रसंघनन, जुरासिक, जारा डोम, कच्छ, गुजरात।

INTRODUCTION

THE Kachchh Basin is a pericratonic basin which formed on the western margin of the Indian Plate (Biswas, 1991). The Mesozoic sediments in this basin are exposed in the form of six discontinuous domal areas; (a) Kachchh Mainland, (b) Pachham Island, (c) Khadir Island, (d) Bela Island, (e) Chorar Island and (f) Wagad. These domes are major uplifts forming highlands that are separated by vast covered plain. The Kachchh Mainland rocks belonging to Bajocian to Albian age are exposed in the form of two E–W chains of "Domes", namely, (1) the Northern Flexure Zone (2) and the Katrol Hills range (Biswas, 1993). Lithostratigraphically Kachchh Mainland comprises of Jhurio, Jumara, Jhuran and Bhuj formations in ascending order. The Mainland outcrops are exposed as a continuous succession and consist of most prominent ridge extending for about 193 km from Jawahar Nagar in the east to Jara in the west (Table 1). The total area of the basin is about 16,500 sq. miles of which outcrop area include only 5000 sq. miles. The basin is filled up with 5000 to 8000 ft. of Mesozoic sediments and 1800 ft. of Tertiary sediments. The Mesozoic succession developed due to marine incursions during Middle Jurassic to Early Cretaceous period and was followed upward by the Katrol Formation yielding ammonites of the Kimmeridgian age (Fursich *et al.*, 1991). The Kachchh Basin evolved due to sequential rifting and repeated movements along Precambrian tectonic trends, which took place in relation to the Indian Plate northward drift after breakup of the Gondwanaland in the Late Triassic–Early Jurassic (Norton & Sclater, 1979; Biswas, 1987). Kachchh rifting along the Delhi Trend was initiated in the Late Triassic as evidenced by continental rhaetic sediments in the northern part of the basin (Koshal, 1984). During Jurassic time in the early stages of India's northward drift away from Gondwanaland, the Kachchh rift basin was formed from the subsidence of a block between Nagarparkar Hills and southwest extension of Aravalli Range. The first occurrence of marine sediments in the Middle Jurassic (Bajocian) indicates that the graben became a fully marine basin during that time. In the Early Cretaceous time the basin was filled up and the sea began to recede (Bardan & Datta, 1987). The Late Cretaceous witnessed extensive regional uplift in the western part of India.

In Jara Dome area in northwestern Mainland, the formation is predominantly arenaceous (Fig. 1). It is a quaquaversal Dome 3 km in diameter, bounded by the Northern latitudes of 23°43' to 23°45' and the east longitudes of 68°57' to 69°00'. The Jara Dome is represented by sandstone, shale and limestone. Here the formation has two distinct parts, the upper part is composed mainly of sandstone beds and the lower is composed of alternating beds

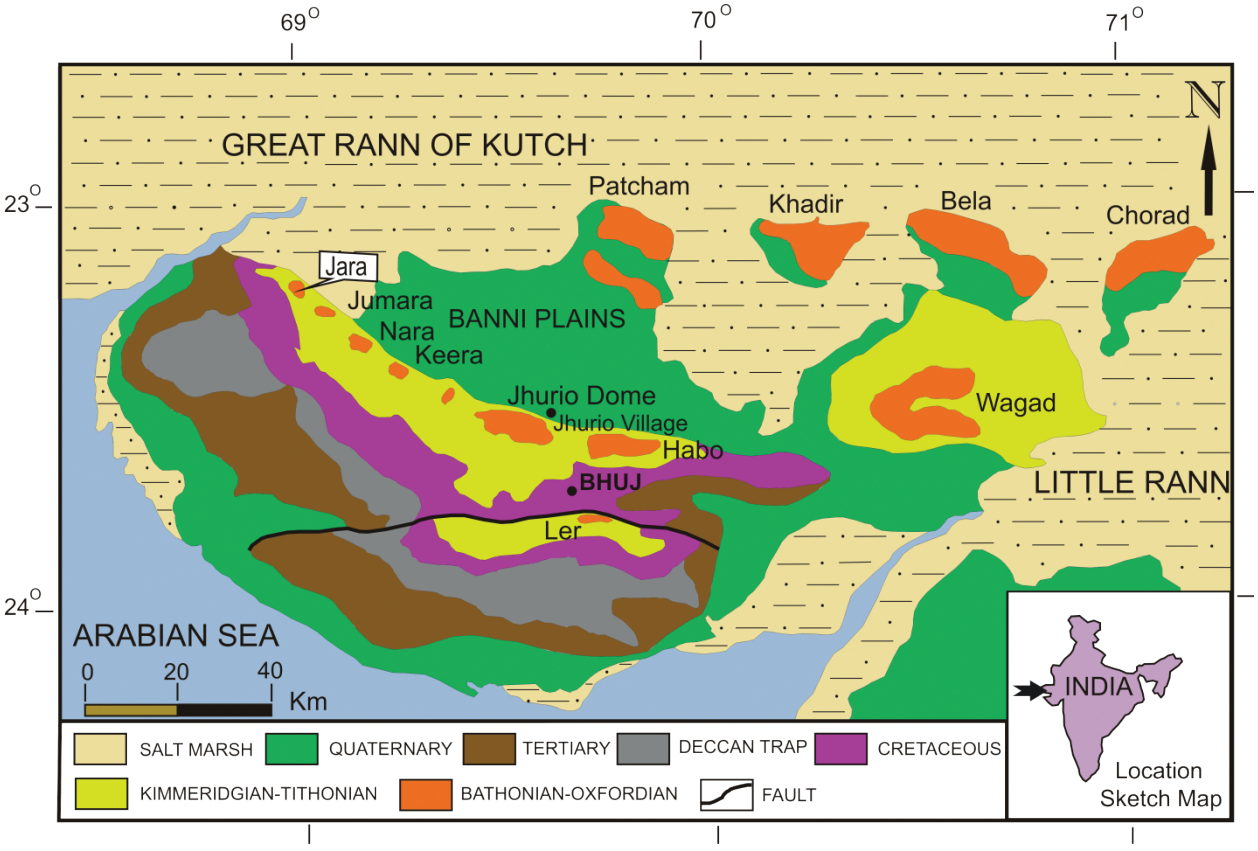

Fig. 1—Geological map of Kachchh Basin (after Biswas SK, 1977).

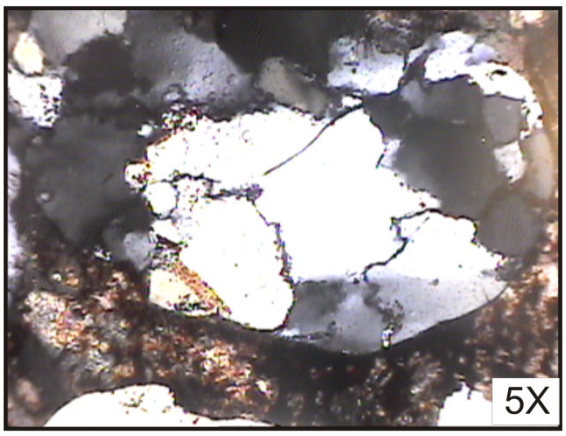

1

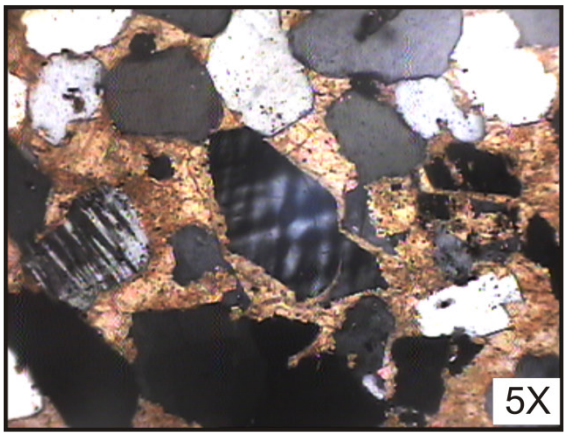

2

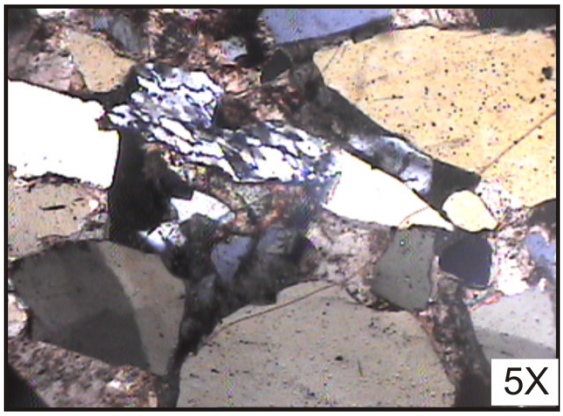

3

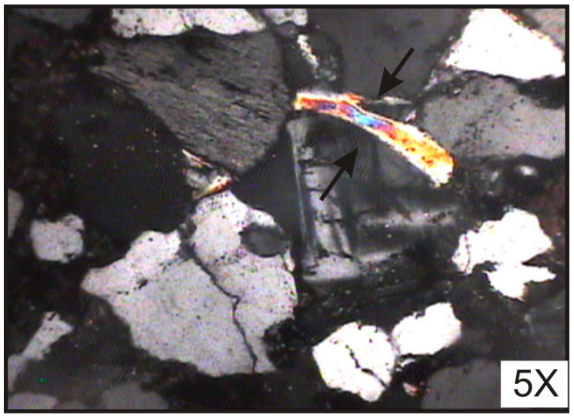

4

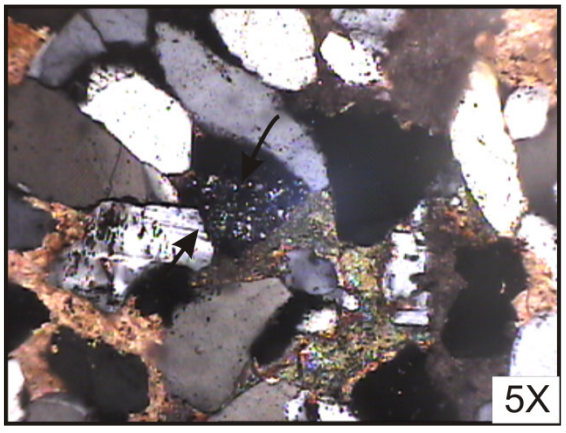

5

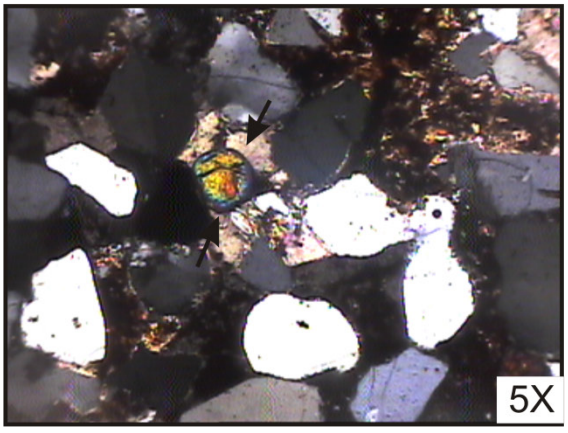

6

PLATE 1

Photomicrographs showing:

1. quartz grain.
2. fresh feldspar grain.
3. weathered feldspar grain.
4. muscovite grain.
5 chert grain.
6 zircon.

of sandstone and shales. The present study provides a first hand detailed report on the petrography and diagenesis of sandstones of Jara Dome in order to evaluate the factor that influence the detrital composition and diagenetic evolution.

GEOLOGICAL SETTING

The Kachchh marine Jurassic rocks deposited in an extensive area of Tethys at the northwestern corner of the Indian Plate are particularly well known for their mega fossils. The Kachchh Basin formed due to rifting and counter–clockwise rotation of the Indian Plate in the Late Triassic/early Jurassic (Biswas, 1987). Two factors that controlled basin–fill sediment accommodation are tilting of fault blocks and sea level stand during deposition . The Kachchh Mesozoic rift is a global example of rift fill sedimentation. The Mesozoic sediments comprise Late Triassic to Early Jurassic continental, Middle to Late Jurassic marine and Late Jurassic to Early Cretaceous fluvio–deltaic sediments. The basin fill consists predominantly of shallow–water (mainly sandy) to basinal (mainly clayey–silty) siliciclastics, deposited on a ramp; carbonates are insignificant, except for the Late Bathonian. Locally shoals consisting of ferruginous ooids existed in the Bathonian and Callovian and are found interspersed between the carbonates or siliciclastics. Sedimentary environments range from deltas to nearshore bars, protected embayments, storm dominated shelf and shallow basins beyond storm influence.

MATERIAL AND METHODS

Thirty five samples were collected from two measured sections–Dam section and Nala section of the Jara Dome, Kachchh (Fig. 2). All the collected sandstone samples were cut and made into thin sections for detailed petrographic and diagenetic studies using a polarizing microscope. In order to reconstruct the original detrital composition of sandstones, the effects of diagenesis were taken into consideration as much as possible during counting. The heavy mineral identification was undertaken following (Krumbein & Pettijohn, 1938; Milner, 1962). The nature of detrital grain contacts were studied and classified after Taylor (1950). For computation of Contact Index, the method of Pryor (1973) was employed.

DETRITAL MINERAL COMPOSITION

The Ridge and Athleta sandstones are thick to thin bedded, whitish to reddish brown, medium to coarse grained, moderately to well sorted. The grains are subangular to subrounded with low to medium spherecity. Tabular, trough cross–bedding, laminations and wavy bedding are common. The sandstones are texturally and compositionally mature. Scattered quartz pebbles are encountered at places.

The average composition of detrital minerals of sandstones is: quartz 86.59%; feldspar 9.37%; mica 2.34%; chert 0.69%; rock fragments 0.74% and heavy minerals 0.26%. Ridge Sandstone of Chari Formation is represented by 86.85% quartz; 8.63% feldspar; 2.65% mica; 0.59% chert; 0.89% rock fragments and 0.31% heavy minerals. Athleta Sandstone of Chari Formation consist of 86.59%

Formation	Member	Age
Umia Formation	Bhuj	Albian
	Ukra	Aptian
	Ghuneri	Neocomian
	Umia	Tithonian
Katrol Formation		Tithonian–Kimmerdgian
Chari Formation	Dhosa Oolite	Late Early Oxfordian
	Dhosa Sandstone Member	Early Oxfordian
	Gypsiferous Shale Member	
	Athleta Sandstone Member	
	Ridge Sandstone Member	
	Shelly Shale/Keera	Callovian
	Golden Oolite	
Patcham Formation	Sponge Limestone	Bathonian
Jhurio Formation	–	Bathonian–Bajocian

Table 1—Lithostratigraphic framework of the Jurassic and Lower Cretaceous rocks of Kachchh Mainland (after Fursich *et al.*, 1991, 1992, 2001).

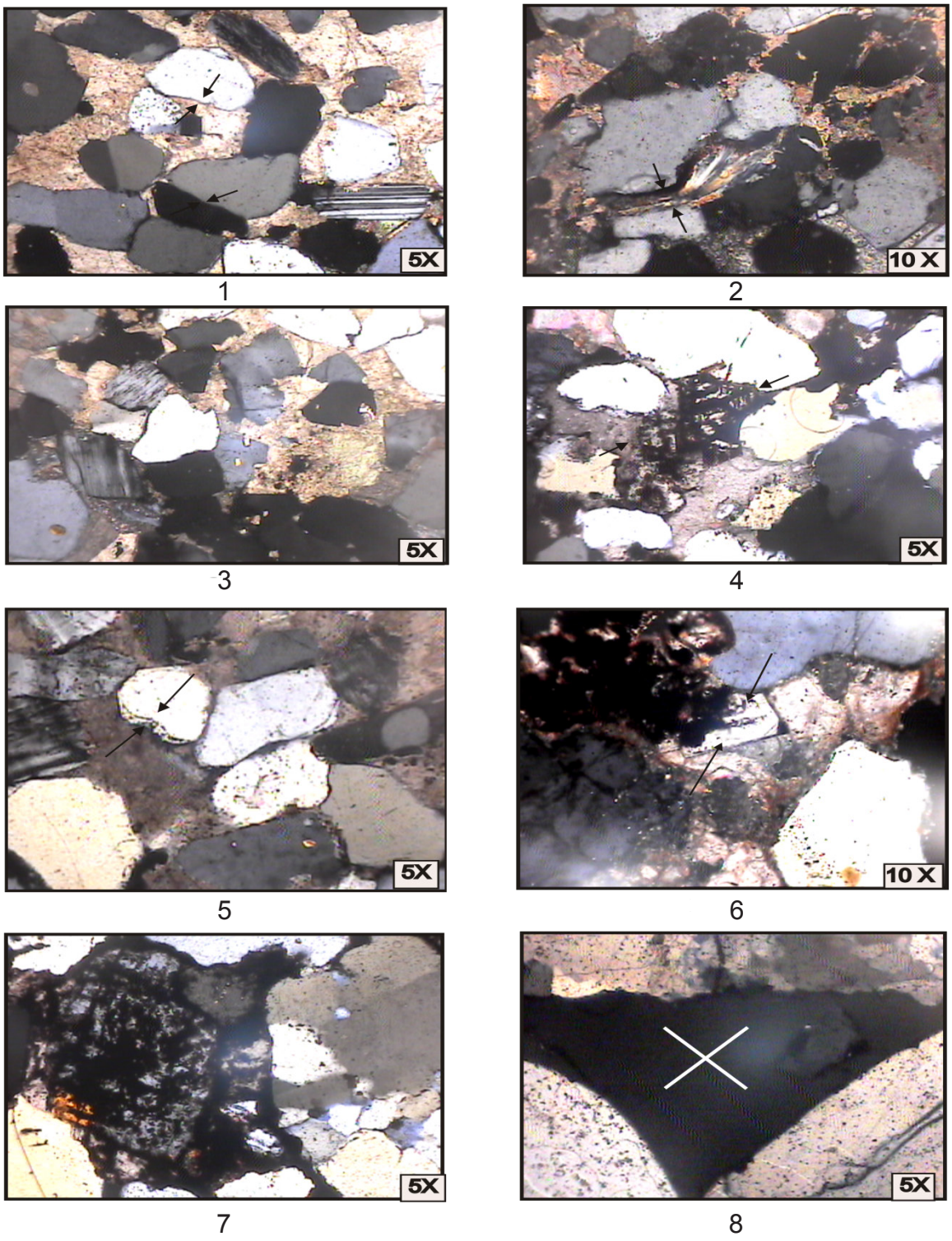

PLATE 2

Photomicrographs showing:

1. point, long and concavo–convex contacts.
2. effect of compaction.
3. detrital grains corroded by carbonate cement.
4. feldspar grain corroded by iron cement.
5. silica overgrowth.
6. dolomite cement.
7. clay cement.
8. secondary porosity.

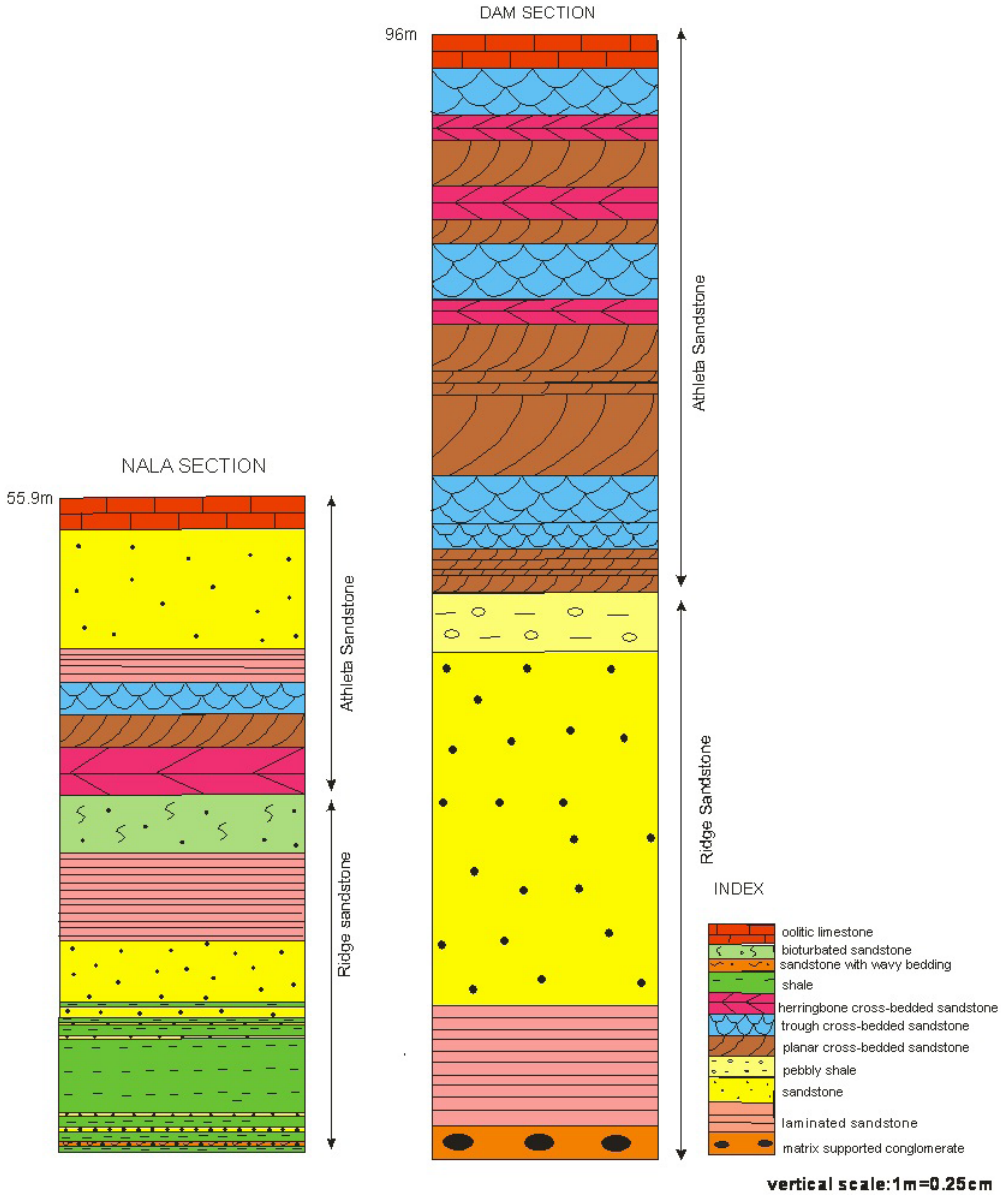

Fig. 2—Lithostratigraphic sections of Jara Dome.

quartz, 9.37% feldspar, 2.34% mica, 0.69% chert, 0.74% rock fragments and 0.26% heavy minerals (Table 2, Plate 1.1–6). Heavy minerals include opaques, tourmaline, zircon, rutile, garnet, staurolite and biotite. The detrital constituents were recalculated to 100 percent excluding clay matrix, authigenic cement having mineral and micas. The studied samples mainly fall in quartzarenite and subarkose fields.

FACTORS CONTROLLING DETRITAL MINERALOGY

Palaeoclimate, distance of transport, source rock composition and diagenesis are the most important factors controlling the composition at the time of deposition. These factors were studied in detail in order to analyze their effect on detrital composition.

Palaeoclimate

Bivariant log/log plot of the ratio of polycrystalline quartz to feldspar plus rock fragments (Suttner & Dutta, 1986) has been used for interpreting the palaeoclimate of Ridge and Athleta sandstones. The mean value of the ratio were plotted (Fig. 3) and these indicate humid climate for the area .

The precipitation of large amount of carbonate during Jurassic is also supportive of the fact that the area was witnessing warm climate similar to found in tropics. A combination of low relief, hot humid climate and ample

vegetation can produce quartz rich detritus (Franzinelli & Potter, 1983). Low relief provides prolonged residence time of sediments, thereby increasing the detritus of chemical weathering and thus the sediments rich in the stable quartz. Thus, climate might have been an important factor in the production of compositionally mature quartz rich sandstones. However, climate alone cannot produce quartz rich sands.

Source Rock Composition

The suite of heavy minerals present in the studied sandstones including biotite, tourmaline and zircon indicates an acid igneous source for these sandstones. The dominant alkali feldspar encountered in this study is microcline, which indicates a granite and pegmatite source. On the other hand the suite of heavy minerals including garnet, staurolite reflects a metamorphic source. However, the occurrence of various shades of garnet indicates different source rocks from acid igneous to metamorphic rocks. The suite of heavy minerals, including rounded grains of tourmaline, rutile and zircon is indicative of the reworked source for these sandstones. These heavy mineral suites in the Ridge and Athleta sandstones reflect their source in a mixed provenance, such as believed to represent the eroded and weathered parts of the present day Aravalli Range situated east and northeast of the basin and Nagarparkar Massif situated to the north and northwest (Dubey & Chatterjee, 1997).

Distance of Transport

The detrital grains of the Ridge and Athleta sandstones are in sand size range and derived from Aravalli Range that suggests transportation for a distance of few hundred kilometers. The studied sandstones show small amount of feldspar and one possible reason for this deficiency may be the transportation of sediments by high gradient streams and rapid destruction of feldspar by abrasion. Since deposition of Ridge and Athleta sandstones took place in a tectonically active rift, presence of high gradient stream is quite likely within the basin. However this premise does not stand to scrutiny because rock fragments which could have been destroyed more easily are common within studied sandstones. Therefore, some factors other than transportation were responsible for paucity of feldspar in both the studied sandstones. Feldspar are removed to large extent in humid climatic condition by chemical weathering.

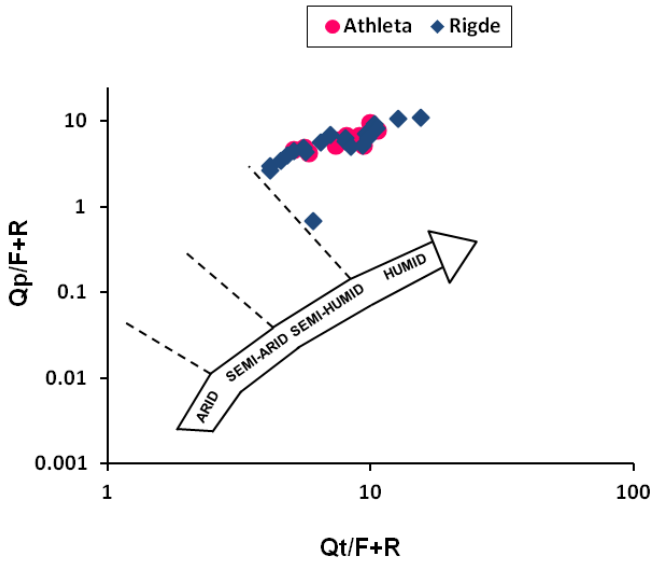

Fig. 3—Bivariant log/log plot for Jara Dome sandstones, Kachchh Basin, according to Suttner & Dutta (1986).

Diagenetic Modification

The diagenetic modifications in the Ridge and Athleta sandstones include loss of detrital framework grains by dissolution, alteration of grains by replacements or by recrystallization and the loss of identity of certain ductile grains. The process of replacement is effective in modifying the detrital composition of sandstones. The replacements of quartz by carbonate and iron oxide cement in the studied sandstones suggest modification of the composition of the sandstones. The study of grain contacts of the sandstones indicates that the sandstones were subjected to compaction during burial and their original texture and fabric was slightly modified by the processes of compaction.

COMPACTION

Various types of grain to grain contacts were point counted in 35 thin sections (Plate 2.1) with a view to estimating pore space reduction as a result of compaction. The average grain contacts include: Floating grains (Ridge Sandstone 41.8%; Athleta Sandstone 36.2%), Point contacts (Ridge Sandstone 31.7%; Athleta Sandstone 36.95%), Long contacts (Ridge Sandstone 17.8%; Athleta Sandstone 20.3%); concavo–convex contacts (Ridge Sandstone 3%; Athleta Sandstone 2.85%) and sutured contacts (Ridge Sandstone 3%; Athleta Sandstone 1.1%) (Table 3).

The overall average contact index for the Ridge and Athleta sandstones is very low. The framework grains having contacts with 1–4, and more than four grains constitute about 43.53, 32.93, 14.6, 2.73, 2.06, 40.75, 32.3, 18, 4.9, 1.25, respectively (Table 3). It is well known that the original porosity of sandstones generally vary between 30 and 50%, which can be reduced by 10–17% by mechanical compaction (Pryor, 1973; Beard & Weyl, 1973). The initial high porosity is attributed to loose packing of sediments at the onset of deposition. In addition to compression, rotation of the grains and their mechanical breakage during burial also reduces porosity in sandstones (Plate 2.2). The Ridge and

Athleta sandstones members exhibit distinct cement–grain boundaries in a few samples. The intergranular quartzose cement (minus cement porosity) in these cases averages 27, 26.67 % respectively, which may be due to less mechanical compaction during the early stages of diagenesis. Less mechanical compaction and high content of intergranular cement may be related to high grain strength, good sorting and early cementation.

CEMENT AND MATRIX

Six types of cements were identified in the Ridge and Athleta sandstones including carbonate, iron oxide, silica, clay, dolomite and glauconite (Table 4).

Carbonate Cement

The carbonate cement in the studied sandstones occur in the form of sparry calcite and microcrystalline calcite cements. Some detrital grains have been dissolved and replaced by calcite cement. Both quartz and feldspar grains have been corroded and replaced by carbonate. The original framework of the sandstones has been modified as a result of replacement of detrital grains by carbonate cement (Plate 2.3). The replacement cementation clearly implies that pore waters were under–saturated with respect to quartz and supersaturated with respect to calcite. Quartz was corroded by the continued movements of fluids. In some thin sections characterised by Fe–calcite cement corroded the quartz grains exhibit calcite cement infilling. This evidence suggests the presence of syndepositional calcite cement, which was later replaced by Fe–calcite cement during deep burial. Microcrystalline calcite cementation probably precipitated at shallow depth above water table by the process of concretion as evidenced by open framework entrapped iron–oxide cement; later during burial diagenesis, microcrystalline calcite cement were replaced by sparry calcite in meteoric hydrologic regime along the interface zone of accretion and saturation. The early precipitation of carbonate cement takes place in a few centimeters below the sediment water interface (Bjorlykke, 1983). The carbonate cement formed during burial by dissolution and reprecipitation represents redistributed calcite which was buried with the sandstone. The presence of oversized pore filled calcite cement might be due to destruction and leaching of labile framework grains, possibly feldspar, that may have taken place at sediment–water interface.

Iron Oxide Cement

The iron oxide cement is present in three different forms: first as pervasive pore fillings, second as isolated patches and third as thin coatings around detrital grain boundary. The pervasive development of iron–oxide cement, dark brown in colour, is associated with high percentage of floating grains and oversized pores. In many instances, pervasive iron–oxide cement corrode and replace detrital grains along cleavage and grain boundaries, causing loss of morphology and forming protrusions, embayments and notches (Plate 2.4). The oversized hematite filled pores may either be the result of excessive corrosion and complete digestion of detrital grains or represent an early stage of cementation. The light brown to brown patchy iron oxide distribution suggests either aborted cementation or dissolution during uplift. The iron–oxide cement coating around detrital grains and interparticle pore spaces, present in few samples, is due to release of iron oxide through the disintegration of unstable ferromagnesian minerals during weathering and pedogenic processes. The iron oxide also replaces calcite cement which indicates late stage cementation. The iron oxide cement is perhaps derived from weathering and leaching of ferromagnesian minerals of overlying Deccan Traps (Walker, 1974).

Silica Cement

The silica cement occurs in the form of quartz overgrowth on subangular and subrounded quartz grains floating in carbonate iron oxide cement as well as microcrystalline chalcedony which fill up the pore spaces. The silica overgrowth develops due to precipitation from aqueous solution in optical continuity with the grains, partially filling up the intergranular spaces (Plate 2.5). The source of silica cement may be the descending meteoric water saturated with silica or pressure solution of detrital quartz and other silicates at grain contacts. The conversion of clay minerals during diagenesis and decomposition or alteration of feldspar may release silica saturated solutions. Such solution may also be produced by hydration and leaching of volcanoclasts. Chalcedony precipitated rapidly from concentrated solution of silica whereas in the later stage mega quartz crystallize slowly from dilute solution (Versey, 1939).

Dolomite Cement

Dolomite as cement occurs only in a few samples of sandstone under study. This was identified using staining test and certain optical properties. It occur as of isolated crystals, in patches and as pervasive which forms rhombic crystals (Plate 2.6). Dolomite, in general, is found to replace calcite. It has brown stains and is probably ‘ferroan’. The dolomite rhombs are euhedral to subhedral and abut against framework grains. Such rhombs also exhibit sharply defined zoning with iron–rich and iron–poor composition alteration. Dolomitization normally require, increase in Mg–concentration, high temperature and evaporation, high CO_2 pressure, high Mg/Ca ratio, lower SO_4 and organic acid effects (Tucker & Wright, 1991). Occasionally dolomite cement may form due

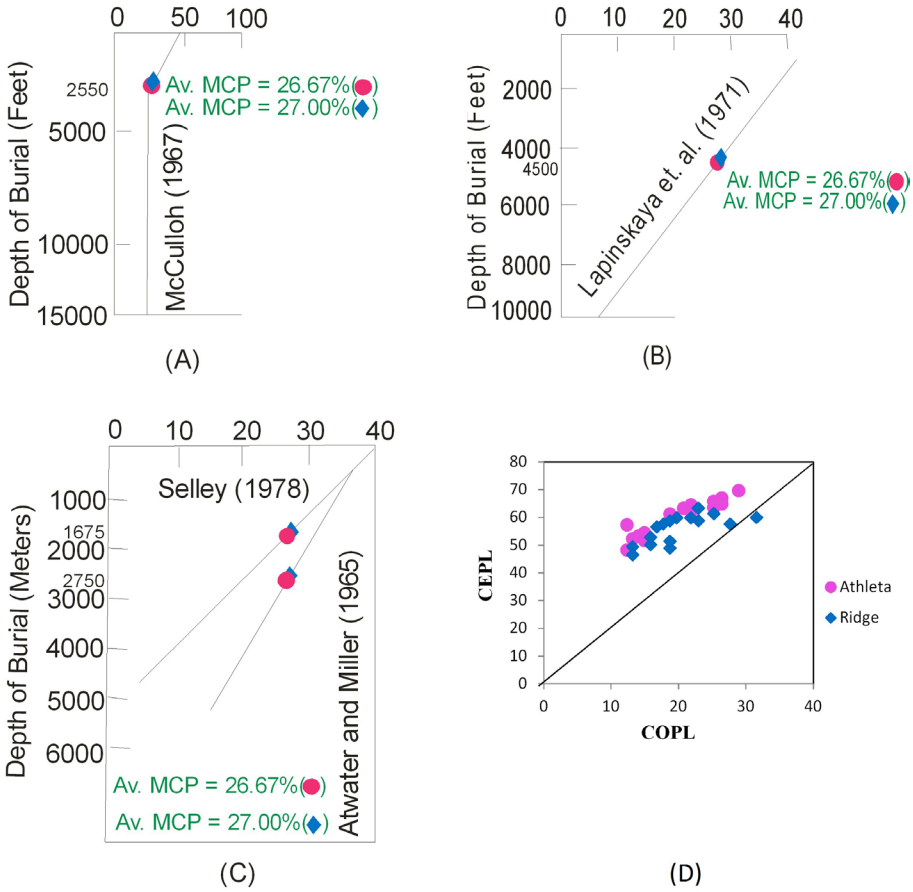

Fig. 4—The relationship between MCP and depth of burial on the three bivariate (A, B, C) determined for Jara Dome sandstones. The plot (D) is of porosity loss due to compaction v/s porosity loss due to cementation

to incursion of surface water, rich in Mg ions, which mix with circulating basinal pore–water (Tucker, 1986; Morse & Wright, 1990).

Clay Cement

The clay cement is present in minor amount. It is mainly kaolinite, chlorite and occurs as intergranular microcrystalline aggregate of both allogenic and authigenic origin (Plate 2.7). The allogenic kaolinite is very common and show irregular aggregate of plates with rugged outlines, often conforming with the adjacent coarser detrital grains, a result of deformation, during compaction. Authigenic kaolinite shows well developed rosettes crystals, not deformed by compaction. They are alteration products of mica and feldspar grains during compaction. Chlorite occurs both as a pore filling mineral and a replacement mineral detrital grains, such as feldspar and calcite cement. Pore filling chlorites appear as rosettes or crystal aggregates within the pores (Rahman *et al*., 2011). Chlorite, also grows tangentially to the surface of detrital grains, forming rosette type structures.

Glauconite Cement

Glauconite cement occurs only in few samples. It occurs in patches between intergranular spaces. Detrital grains are corroded by glauconite cement. A direct relationship existed between the formation of glauconite cement in the Kachchh Basin and physicochemical environment of deposition entirely controlled by the tectonic history of the basin.

Matrix

In the studied sandstones, silty to clayey matrix is present in varying amounts. Both syndepositional and post depositional matrix are present. The matrix also influences diagenetic process by supplying Fe and reducing porosity and permeability by pore filling.

POROSITY EVOLUTION AND DEPTH OF BURIAL

The grain contact and the amount of porosity reduction have been employed to the study of depth burial of Ridge and

S. No.	Monocrystalline Quartz	Polycrystalline Quartz		Feldspar		Mica		Chert	Rock Fragments	Heavies
	Common Quartz	Recrystallized Metamorphic Quartz	Stretched Metamorphic Quartz	Plagioclase	Microcline	Muscovite	Biotite			
Athleta Sandstone Member										
A1	84.02	0.33	1.20	0.00	8.65	2.00	0.00	1.00	1.01	0.56
A2	82.44	1.00	0.77	0.56	10.00	4.11	0.01	1.09	0.11	0.65
A3	72.11	3.50	3.00	1.23	11.56	3.23	0.00	1.34	1.45	0.90
A4	73.05	4.00	0.89	2.00	14.50	5.00	0.00	1.00	0.11	0.11
A5	86.33	1.25	1.45	1.00	5.11	1.22	0.40	0.23	2.00	0.00
A6	87.23	3.50	0.55	1.56	4.97	2.00	0.00	0.54	0.56	0.00
A7	81.34	2.10	0.12	1.50	9.56	1.45	0.11	1.45	1.11	0.10
A8	75.65	5.00	2.00	1.11	10.00	2.46	0.00	0.33	0.00	0.00
A9	76.45	4.23	1.22	1.78	11.24	2.10	0.10	0.00	1.54	0.00
A10	85.35	2.56	0.30	0.56	4.87	3.09	0.00	0.65	0.00	0.57
A11	85.45	1.45	1.45	0.00	7.49	1.07	0.23	0.00	0.45	0.00
A12	81.66	4.22	1.66	1.22	6.20	1.55	0.00	0.76	0.89	0.32
A13	84.50	3.87	0.54	0.32	8.00	1.43	0.00	0.00	1.08	0.12
A14	83.45	3.02	0.78	0.21	8.89	2.00	0.70	0.87	0.00	0.00
A15	79.45	6.70	2.10	0.11	6.56	1.01	0.00	1.23	0.86	0.67
Avg.	81.38	3.11	1.20	0.87	8.50	2.24	0.10	0.69	0.74	0.26
Ridge Sandstone Member										
R1	88.67	3.09	0.06	0.00	3.45	1.78	0.01	0.81	0.62	0.67
R2	80.00	2.00	1.13	1.45	9.68	1.67	0.00	1.04	0.00	0.00
R3	72.23	2.56	4.87	1.01	11.00	4.45	0.03	2.00	0.04	0.87
R4	75.98	3.98	0.64	0.00	13.23	4.32	0.00	0.37	1.09	0.32
R5	85.56	2.06	1.45	0.65	5.34	2.67	1.45	0.56	0.00	0.00
R6	83.66	1.34	1.32	0.82	7.03	2.00	0.00	1.24	0.86	0.00
R7	85.00	0.06	0.04	0.05	9.00	5.01	0.00	0.00	0.00	0.09
R8	74.03	2.43	3.00	1.22	11.04	4.09	0.00	1.03	1.54	0.90
R9	75.35	3.21	0.11	1.13	14.65	3.98	0.00	1.88	0.00	0.00
R10	86.16	2.14	1.56	0.45	4.85	2.00	0.00	0.06	2.00	0.02
R11	86.50	1.30	1.61	0.50	4.77	2.23	0.00	0.00	2.10	0.78
R12	78.09	4.39	0.00	1.14	10.45	1.54	0.01	0.45	1.50	0.69
R13	85.45	3.06	0.05	0.56	7.47	1.12	0.00	0.00	1.67	0.01
R14	83.11	4.56	0.00	0.00	5.56	3.56	0.34	0.00	0.50	0.00
R15	81.00	6.98	2.30	0.02	5.67	1.04	0.00	0.87	0.78	0.56
R16	76.17	6.55	1.12	1.67	10.63	2.87	0.78	0.00	0.23	0.00
R17	80.00	3.02	1.73	1.89	7.34	1.66	0.00	0.77	2.00	0.54
R18	86.56	4.12	1.78	0.00	3.09	1.59	0.00	0.01	1.98	0.00
R19	79.09	5.03	1.34	1.32	8.67	1.04	0.00	0.00	1.00	0.67
R20	84.66	6.00	0.00	0.72	5.09	1.09	0.82	0.87	0.00	0.22
Avg.	81.36	3.39	1.20	0.73	7.90	2.48	0.17	0.59	0.89	0.31

Table 2—Percentages of Detrital minerals in the sandstones of Jara Dome, Kachchh, Gujarat.

S.No.	Types of Contacts					Number of Contact per Grain					Total Number of Contacts	Contact Index
	Floating	Point	Long	Concavo-convex	Sutured	0	1	2	3	≥4		
Athleta Sandstone Member												
A1	30.00	50.00	16.00	1.00	0.00	35.00	46.00	11.00	2.00	1.00	60.00	1.00
A2	25.00	45.00	19.00	4.00	1.00	32.00	40.00	18.00	5.00	1.00	64.00	1.31
A3	64.00	15.00	10.00	0.00	0.00	59.00	30.00	8.00	2.00	0.00	40.00	0.78
A4	31.00	30.00	24.00	6.00	1.00	34.00	32.00	20.00	6.00	5.00	63.00	1.10
A5	52.00	31.00	12.00	1.00	0.00	53.00	30.00	12.00	2.00	1.00	45.00	0.80
A6	60.00	20.00	17.00	3.00	0.00	56.00	24.00	11.00	1.00	1.00	37.00	1.06
A7	40.00	40.00	15.00	2.00	0.00	42.00	26.00	16.00	6.00	5.00	53.00	1.40
A8	45.00	24.00	20.00	2.00	0.00	45.00	35.00	14.00	0.00	0.00	49.00	1.01
A9	31.00	42.00	22.00	4.00	1.00	33.00	30.00	24.00	7.00	6.00	67.00	1.61
A10	36.00	26.00	18.00	10.00	1.00	40.00	35.00	16.00	3.00	0.00	54.00	1.33
A11	40.00	38.00	17.00	3.00	0.00	41.00	42.00	12.00	0.00	4.00	58.00	1.13
A12	35.00	40.00	18.00	3.00	2.00	37.00	36.00	15.00	2.00	2.00	55.00	1.35
A13	51.00	24.00	16.00	5.00	0.00	60.00	28.00	9.00	0.00	0.00	37.00	0.78
A14	40.00	24.00	21.00	9.00	1.00	36.00	31.00	20.00	4.00	2.00	57.00	1.53
A15	47.00	27.00	22.00	3.00	0.00	50.00	29.00	13.00	2.00	3.00	47.00	1.01
Avg.	43.75	33.21	18.63	3.90	0.48	43.53	32.93	14.60	2.73	2.06	52.40	1.14
Ridge Sandstone Member												
R1	50.00	29.00	10.00	5.00	2.00	52.00	28.00	10.00	4.00	4.00	46.00	1.00
R2	26.00	49.00	22.00	0.00	0.00	32.00	45.00	16.00	3.00	0.00	64.00	1.11
R3	40.00	39.00	17.00	2.00	0.00	50.00	29.00	13.00	3.00	1.00	46.00	1.05
R4	45.00	33.00	20.00	0.00	1.00	53.00	27.00	18.00	0.00	0.00	45.00	0.90
R5	31.00	36.00	23.00	4.00	0.00	50.00	23.00	19.00	3.00	1.00	46.00	1.20
R6	30.00	34.00	26.00	5.00	2.00	35.00	30.00	26.00	8.00	2.00	66.00	1.55
R7	40.00	38.00	15.00	4.00	0.00	41.00	32.00	17.00	4.00	1.00	54.00	1.35
R8	26.00	44.00	25.00	0.00	0.00	28.00	43.00	17.00	9.00	3.00	72.00	1.46
R9	37.00	36.00	13.00	5.00	4.00	40.00	35.00	13.00	6.00	0.00	54.00	1.41
R10	41.00	37.00	24.00	0.00	0.00	43.00	32.00	19.00	3.00	0.00	54.00	1.35
R11	41.00	39.00	11.00	3.00	3.00	45.00	31.00	13.00	5.00	2.00	51.00	1.30
R12	30.00	46.00	23.00	1.00	0.00	32.00	42.00	18.00	6.00	0.00	66.00	1.31
R13	46.00	36.00	13.00	1.00	0.00	52.00	27.00	14.00	4.00	1.00	46.00	1.10
R14	42.00	34.00	22.00	0.00	1.00	47.00	30.00	20.00	2.00	3.00	55.00	1.20
R15	37.00	32.00	22.00	4.00	0.00	37.00	26.00	22.00	6.00	0.00	54.00	1.50
R16	26.00	36.00	28.00	5.00	1.00	32.00	30.00	26.00	7.00	2.00	65.00	1.51
R17	37.00	35.00	21.00	7.00	4.00	42.00	30.00	18.00	5.00	1.00	54.00	1.31
R18	30.00	37.00	31.00	0.00	0.00	34.00	40.00	21.00	7.00	0.00	68.00	1.42
R19	35.00	36.00	11.00	9.00	0.00	36.00	33.00	16.00	7.00	3.00	59.00	1.46
R20	34.00	33.00	29.00	2.00	4.00	34.00	31.00	24.00	6.00	1.00	62.00	1.62
Avg.	37.16	37.93	20.84	2.92	1.12	40.75	32.20	18.00	4.90	1.25	56.35	1.30

Table 3—Percentages of various types of grain to grain contacts of the sandstones of Jara Dome, Kachchh, Gujarat.

S.No.	Cements						Total Cement	Detrital Grain	Existing Optical Porosity	Minus Cement Porosity	COPL	CEPL
	Silica	Iron	Carbonate		Clay	Matrix						
			Spar	Micrite								
Athleta Sandstone Member												
A1	3.00	9.00	1.00	3.00	0.00	2.00	18.00	79.00	2.00	20.00	13.18	52.38
A2	2.00	13.00	0.00	2.00	1.00	1.00	19.00	75.00	3.00	22.00	14.93	51.77
A3	2.00	15.00	4.00	7.00	3.00	2.00	33.00	60.00	2.00	35.00	28.92	69.70
A4	1.00	11.00	11.00	3.00	2.00	1.00	29.00	65.00	3.00	32.00	25.22	63.64
A5	2.00	12.00	7.00	5.00	0.00	2.00	28.00	70.00	1.00	29.00	21.83	64.53
A6	2.00	10.00	2.00	3.00	1.00	1.00	19.00	80.00	1.00	20.00	12.34	57.34
A7	2.00	10.00	4.00	1.00	2.00	1.00	20.00	75.00	2.00	22.00	14.93	54.48
A8	1.00	10.00	12.00	5.00	1.00	2.00	31.00	64.00	2.00	33.00	26.41	67.08
A9	3.00	10.00	8.00	6.00	1.00	2.00	30.00	64.00	3.00	33.00	26.41	64.92
A10	2.00	8.00	8.00	8.00	0.00	1.00	27.00	70.00	2.00	29.00	21.83	62.22
A11	2.00	7.00	1.00	4.00	1.00	1.00	16.00	80.00	3.00	19.00	12.34	48.28
A12	1.00	11.00	0.00	3.00	2.00	2.00	19.00	75.00	2.00	21.00	14.05	53.43
A13	1.00	10.00	6.00	8.00	3.00	2.00	30.00	64.00	2.00	32.00	25.21	65.84
A14	2.00	7.00	7.00	6.00	1.00	2.00	25.00	72.00	1.00	26.00	18.71	61.28
A15	2.00	7.00	7.00	9.00	0.00	2.00	27.00	70.00	1.00	28.00	20.75	63.41
Avg.	1.40	9.13	5.20	4.86	0.66	1.20	24.73	70.86	2.00	26.67	19.87	60.02
Ridge Sandstone Member												
R1	3.00	16.00	0.00	1.00	4.00	5.00	29.00	61.00	8.00	37.00	31.58	60.02
R2	2.00	18.00	1.00	0.00	3.00	3.00	27.00	65.00	7.00	34.00	27.65	57.69
R3	1.00	21.00	0.00	0.00	2.00	4.00	28.00	70.00	2.00	30.00	22.93	63.40
R4	1.00	21.00	0.00	1.00	0.00	2.00	25.00	71.00	2.00	28.00	19.73	59.93
R5	1.00	18.00	1.00	2.00	2.00	2.00	26.00	70.00	3.00	29.00	21.83	59.92
R6	2.00	16.00	0.00	1.00	2.00	1.00	22.00	73.00	2.00	24.00	16.77	56.62
R7	2.00	14.00	0.00	0.00	0.00	1.00	17.00	80.00	3.00	20.00	13.18	49.45
R8	3.00	13.00	1.00	2.00	1.00	2.00	22.00	73.00	2.00	24.00	16.77	56.62
R9	1.00	10.00	2.00	0.00	1.00	2.00	16.00	80.00	4.00	20.00	13.18	46.54
R10	2.00	12.00	0.00	1.00	3.00	2.00	20.00	71.00	6.00	26.00	18.71	49.00
R11	2.00	10.00	0.00	0.00	2.00	5.00	19.00	73.00	4.00	23.00	15.83	50.25
R12	1.00	19.00	0.00	3.00	1.00	4.00	28.00	64.00	4.00	32.00	25.22	61.44
R13	2.00	20.00	1.00	1.00	2.00	2.00	28.00	70.00	2.00	30.00	22.92	63.39
R14	2.00	18.00	0.00	0.00	1.00	3.00	24.00	72.00	2.00	26.00	18.71	58.80
R15	2.00	18.00	1.00	2.00	2.00	1.00	26.00	70.00	3.00	29.00	21.82	59.91
R16	2.00	12.00	2.00	1.00	3.00	3.00	23.00	73.00	2.00	25.00	17.73	57.71
R17	1.00	13.00	0.00	1.00	1.00	6.00	22.00	75.00	2.00	24.00	16.78	56.63
R18	2.00	11.00	1.00	1.00	3.00	2.00	20.00	76.00	3.00	23.00	15.84	52.91
R19	2.00	10.00	2.00	1.00	2.00	4.00	21.00	72.00	5.00	26.00	18.72	51.46
R20	2.00	16.00	2.00	2.00	1.00	3.00	26.00	70.00	4.00	30.00	22.93	58.87
Avg.	1.75	16.45	0.65	0.85	1.65	3.25	23.45	71.45	3.50	27.00	19.99	56.53

Table 4—Percentages of cement and void spaces of the sandstones of Jara Dome, Kachchh, Gujarat.

Athleta sandstones. The present study is based on graphic plots of porosity versus depth (Fig. 4) The existing optical porosity (EOP) of Ridge Sandstone ranges from 2 to 8 percent with an average of 3.50 percent, while minus cement porosity (MCP) ranges from 28 to 37 percent with an average of 27 percent. The existing porosity of Athleta Sandstone ranges from 1 to 3 percent with an average of 2 percent and minus cement porosity ranges from 19 to 33 percent and average 26.67 percent. The average minus cement porosity of these sandstones are 27 and 26.67 percent and are plotted on different graphs of porosity versus depth after McCulloh (1967), Lapinskaya and Preshpyakove (1971), Selley (1978) and Atwater and Miller (1965) which suggest a depth of burial in the range of 670 to 2600 m and 762 to 2750 m for Ridge Sandstone and Athleta Sandstone respectively (Fig. 4A, B, C; Table 5).

However the upper limit of the depth range is not consistent with the petrographic clues that are indicative of at least intermediate depth of burial but in some cases deep burial for these sandstones. One possible reason for this inconsistency could be the limited number of samples analysed. Another reason could be the dominantly medium grained nature of these sandstones.

The plot COPL (porosity loss due to compaction) versus CEPL (porosity loss due to cementation) plotted on variation diagram given by Lundegard (1992) suggest that cementation was major cause of the porosity reduction (Fig. 4D). High minus cement porosity values also suggest low mechanical compaction probably just before cementation leading to moderate packing (Plate 2.8). The early cementation may have reduced porosity and establish constituent framework, which appears to have restricted late stage compaction during deep burial (Houseknecht, 1987).

DIAGENETIC EVOLUTION

In the studied sandstones, mechanical compaction was operative during early stage of diagenesis, causing rotation and adjustment of grains and formation of point contact. Compaction, largely influenced by roundness of detrital particles was possible in the absence of an early major cementation phase that could have established the detrital framework. Another burial diagenetic event was alteration of feldspars and dissolution. The feldspar grains show different stages of alteration, dissolution and loss of feldspar can take place in the shallow weathering zone or in the deep surface (McBride, 1985). The original porosity of about 30 to 50% were reduced to an average 26.67 and 27% of Chari Formation Mechanical compaction did not give rise to much pressure solution as is evidenced by the absence of limited number of concavo–convex and sutured grain contacts.

Among the various cements, silica cement was the first to be precipitated in the form of overgrowths partially filling the interparticle pore space. The silica forming overgrowth was probably due to intraformational release of silica during replacement and corrosion of feldspars, dissolution of quartz grains and/or from compaction water. Precipitation of calcite took place in the meteoric hydrologic regime. Iron oxide formed last due to weathering and pedogenic processes. Dolomite cement have formed due to incursion of surface water. Authigenic kaolinite was deposited in the available interparticle pore spaces. Kaolinite occur as pore fillings surrounded by calcite and iron oxide cements. Finally, chalcedony precipitated rapidly from concentrated solution of silica, whereas in the later stages megaquartz crystallized slowly from dilute solutions (Versey, 1939).

Overall diagenetic history of Ridge and Athleta sandstones (grain contacts, minus cement porosity, porosity reduction) indicate intermediate to deep burial conditions for these sandstones. The first phase of diagenesis consisted of mechanical compaction and precipitation of small amounts of quartz cement. The second phase of diagenesis commenced with pre–Deccan Trap uplift when the uplifted sediments were subjected to weathering and pedogenic processes and flushing by meteoric waters. Interparticle pore spaces were almost completely obliterated by the precipitated of calcite cement and infiltration of clay and iron oxide in the freshwater phreatic zone. However, secondary porosity was generated by dissolution and leaching of feldspar grains, calcite and iron oxide cements. Porosity and permeability were reduced at a later date by deposition of authigenic kaolinite and chlorite in the secondary pore spaces of sandstone units.

Depth of Burial vs Minus Cement Porosity	Ridge Sandstone		Athleta Sandstone	
	feet	metre	feet	metre
McCulloh (1967)	2200	670	2500	762
Lapinskaya and Preshpyakove (1971)	4550	1386	4600	1402
Selley (1978)	5741	1750	5905	1800
Atwater and Miller (1965)	8530	2600	9022	2750

Table 5—Interpreted depth of burial of the Ridge and Athleta Sandstone of Jara Dome, Kachchh Basin, Gujarat.

CONCLUSIONS

The Ridge and Athleta Sandstones of Jara Dome are medium to coarse grained, subangular to subrounded and moderately to well sorted. The dominant framework constituents of these sandstones are quartz, feldspar, rock fragments and micas. These sandstones are quartzarenitic and subarkose.

The mineralogical composition of these sandstones reflects their source in the mixed provenance that includes plutonic basement, sedimentary and metasedimentary rocks. The provenance is believed to represent the eroded and weathered parts of the present day Aravalli Range situated east and northeast of the basin and Nagarparkar Massif situated to the north and northwest.

The nature of various types of grain contacts suggests early cementation and consequent minor compaction. The original porosity is about 45% and average minus cement porosity of 27 and 26.67% suggests that, little compaction has taken place. The sandstones were cemented soon after deposition and prior to chemical compaction. Cementation of these sandstones appears to have been initiated with silica, followed by calcite, Fe–calcite (oxide), dolomite, glauconite and clay.

Types of grain contacts, minus cement porosity, porosity reduction, formation of suture and line boundaries indicate intermediate to deep burial conditions for theses sandstones. However, different graphs of porosity versus depth suggest depth of burial in the range of (670–2600 m for Ridge Sandstone; 762–2750 m in case of Athleta Sandstone), which is not consistent with petrographic evidence that instead suggest intermediate to deep burial. The discrepancy is possible due to the limited number of samples analyzed and also dominantly medium grained nature of these sandstones.

Acknowledgements*—The authors gratefully thank the Chairman, Department of Geology, Aligarh Muslim University, Aligarh for providing the necessary research facilities.*

REFERENCES

Atwater GI & Miller EG 1965. The effects of decrease in porosity with depth on future development of oil and gas reserves in south Louisiana. Bulletin of the American Association of Petroleum Geologists 49: 622–626.

Bardan S & Datta K 1987. Biostratigraphy of Jurassic Chari Formation, A study in Keera dome, Kutch, Gujarat. Journal of Geological Society of India 30: 121–131.

Beard DC & Weyl PK 1973. Influence of texture on porosity and permeability of unconsolidated sand. Bulletin of the American Association of Petroleum Geologists 57: 349–369.

Biswas SK 1987. Regional tectonic framework, structure and evolution of the western marginal basins of India. Tectonophysics 135: 307–327.

Biswas SK 1991. Stratigraphy and sedimentary evolution of the Mesozoic Basin of Kutch, western India. *In*: Tandon SK, Pant CC & Cashyap SM (Editors)—Stratigraphy and sedimentary evolution of western India: 74–103. Gyanodaya Prakashan, Nainital.

Biswas SK 1993. Geology of Kutch. K.D. Malaviya Institute of Petroleum Exploration, Dehradun.

Bjorlykke K 1983. Diagenetic reactions in sandstones. *In*: Parker A & Sellwood BW (Editors)—Sediment Diagenesis: 169–213. Reidel Publishing, Holland.

Dubey N & Chatterjee BK 1997. Sandstones of Mesozoic Kachchh basins: their provenance and basinal evolution. Indian Journal of Petroleum Geology 6: 55–58.

Franzinelli E & Potter PE 1983. Petrology, chemistry and texture of modern river sands, Amazon River system. Journal of Geology 91: 23–39.

Fursich FT, Oschmann W, Jaitely AK & Singh IB 1991. Faunal response to transgressive and regressive cycles–examples from Jurassic of western India. Palaeogeography Palaeoclimatology Palaeoecology 85: 149–159.

Houseknecht DW 1987. Assessing the relative importance of compaction processes and cementation to reduction of porosity in sandstones. Bulletin of the American Association of Petroleum Geologists 71: 633–642.

Koshal VN 1984. Differentiation of Rhaetic sediments in the subsurface of Kutch based on palynofossils. Petroleum Asia Journal 7: 102–105.

Krumbein WC & Pettijohn FJ 1938. Manual of the Sedimentary Petrology, Appleton Centaury, 549p.

Lapinskaya TA & Preshpyakove BK 1971. Problem of reservoir rocks during exploration for oil and gas at depths. *In*: Sideranko AV (Editor)—Status and Problem: 115–121.

Lundegard FD 1992. Sandstone porosity loss a big picture view of the importance of compaction. Journal of Sedimentary Petrology 62: 250–260.

McBride EF 1985. Diagenetic processes that effects provenance determination in sandstone. *In*: Zuffa GG (Editor)—Provenance of Arenites: 95–114. Reidel, Dordrecht–Boston–Lancaster.

McCulloh TH 1967. Mass properties of sedimentary rock and gravimetric effects of petroleum and natural gas reservoirs. US Geological Survey Professional Paper 528A: 1–50.

Milner HB 1962. Sedimentary Petrography Part II. George Allen and Unwin Ltd.London 715p.

Morse JW & Wright VP 1990. Geochemistry of Sedimentary Carbonates, Elsevier, Armsterdam, 707p.

Norton IO & Sclater JG 1979. A model for the evolution of the Indian Ocean and the breakup of Gondwanaland. Journal of Geophysical Research 84: 6803–6830.

Pryor WA 1973. Permeability–porosity patterns and variations in some Holocene sand bodies. Bulletin of the American Association of Petroleum Geologists 57: 162–189.

Rahman MJJ, McCann T, Abdullah R & Yeasmin R 2011. Sandstone diagenesis of the Neogene Surma Group from the Shahbazpur gas field, Southern Bengal Basin, Bangladesh. Australian Journal of Earth Sciences 104/1: 114–126.

Selley RC 1978. Porosity gradients in North Sea oil bearing sandstones. Journal of Geological Society of London 135: 119–132.

Suttner LJ & Dutta PK 1986. Alluvial sandstones composition and paleoclimate, I. framework mineralogy. Journal of Sedimentary Petrology 56: 329–345.

Taylor JM 1950. Pore space reduction in sandstone. Bulletin of the American Association of Petroleum Geologists 34: 710–716.

Tucker ME 1986. Sedimentary Petrology: An Introduction. Blackwell Scientific, Oxford 252p.

Tucker ME & Wright PV 1991. Carbonate Sedimentology. Blackwell Scientific, Oxford 482p.

Versey HC 1939. The petrography of Permian rocks in the southern part of the Vale of Eden. Quarternary Journal of Geological Society of London 73: 237–242.

Walker TR 1974. Formation of red beds in moist tropical climate: A hypothesis. Geological Society of American Bulletin 84: 633–638.